

# R/G/B Micro-LEDs for In-pixel Integrated Arrays and Temperature Sensing

Yibo Liu\*, Ke Zhang\*, Feng Feng\*, Zhaojun Liu\*\*, Hoi Sing Kwok\*

\*Hong Kong University of Science and Technology, Hong Kong, China

\*\*Southern University of Science and Technology, Shenzhen, China

Multi-functional displays, which can simultaneously do display abilities and environment/ system monitoring, would enable improved user life and device maintenance. Micro light-emitting diodes (Micro-LEDs) are a next generation display platform.<sup>1-4</sup> The Micro-LEDs fabricated from inorganic crystalline semiconductors have become the focus of display research because of their excellent characteristics, such as short response time, low power consumption, high brightness and high stability, and long lifetime.

In these days, with increasing demands for complex, multifunctional electronics in compact, lightweight format, multifunctionality are a major trend in optoelectronics, requiring light-emitting, light harvest, sensing performance, light communications, and etc.<sup>5-7</sup> The high reliability/stability and ultra-fast response time of GaN-/AlGaInP-based Micro-LEDs have been explored as the potential platform of the multifunctional optoelectronic devices in various applications such as visible light communication and sensors.

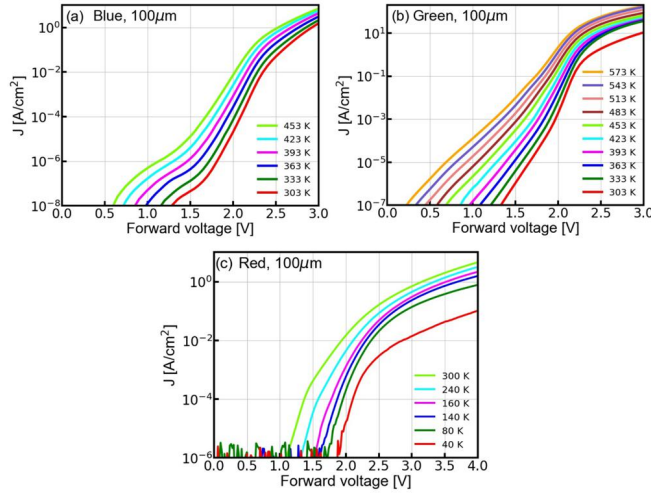


**Fig. 2.** Temperature-dependent J-V curves of (a) blue, (b) green InGaN MQW Micro-LEDs, and (c) red AlGaInP MQW Micro-LED in semi-log scale. The size of three devices is  $100 \times 100 \mu\text{m}^2$ .

The electrical characteristics of R/G/B Micro-LEDs were analyzed by the I-V measurements performed for the wide temperature range. As temperature increases, forward voltage decreases and current density ( $J$ ) increases. The detailed analysis and studies for the electrical characteristics of the J-V curves are beyond the scope of this paper and will be published in another paper shortly. We focus on their temperature-dependent behaviors for temperature sensing.

The ideal behavior of a p-n junction diode is described by the Shockley ideal diode equation:

$$I = I_s \left( e^{\frac{qV}{nk_B T}} - 1 \right)$$

where  $I$  is the diode current,  $I_s$  is the reverse bias saturation current,  $q$  is the charge,  $V$  is the voltage across the diode,  $k_B$  is the Boltzmann's constant,  $n$  is the ideality factor of the diode,

and  $T$  is the absolute temperature. For  $I \gg I_s$ , Eq. (1) give a linear relation between forward voltage and temperature,  $V = AT + B$ , at constant current, where  $A$  and  $B$  are constants obtained from experiments at constant current and calibrated for the target temperature range. The constant  $A$  represent the temperature sensitivity.<sup>8</sup>

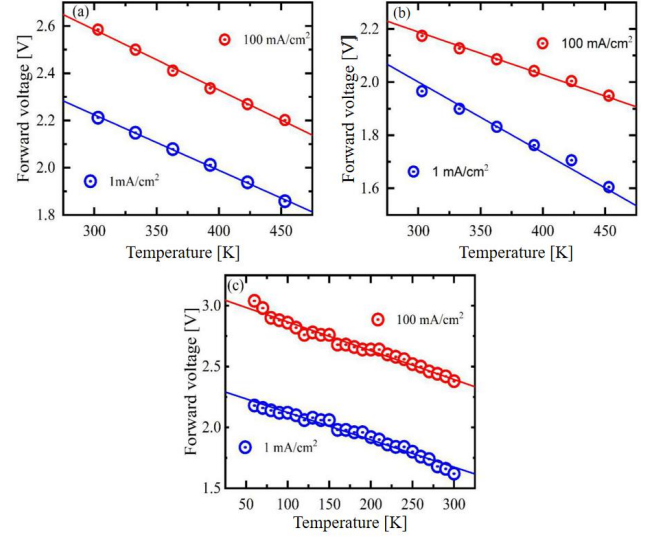


**Fig. 2.** Temperature dependence of forward voltage of (a) blue, (b) green, and (c) red Micro-LED at current constant mode.

At constant current mode, the measured forward voltages (red and blue circles) for Micro-LEDs displayed in Fig 2. From linear fits (solid lines), the slope corresponding to the temperature sensitivity can be obtained as  $-2.4$  and  $-2.6$  mV/K for blue Micro-LED,  $-2.7$  and  $-1.6$  mV/K for green Micro-LED, and  $-2.24$  and  $-2.37$  mV/K for red Micro-LED at 1 (blue solid line) and 100 (red solid line) mA/cm<sup>2</sup>, respectively. For blue and red Micro-LEDs, the change of current density has the negligible effect on temperature sensitivity. However, for green Micro-LED, higher current density leads to slightly higher sensitivity.

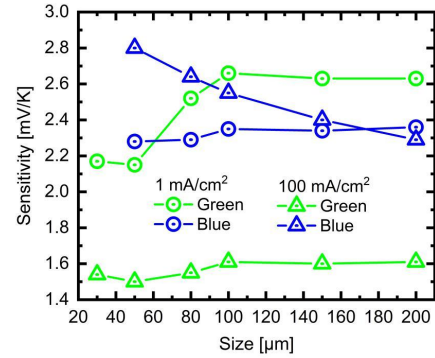


**Fig. 3.** Size dependence of temperature sensitivity for blue and green Micro-LEDs at 1 and 100 mA/cm<sup>2</sup>.

The fabricated blue and green Micro-LEDs do not have the

passivation layer for removing the sidewall damage, which leads to reduced efficiency due to the non-radiative recombination. Due to the large surface-to-volume ratio, efficiency of Micro-LEDs droops with decreasing size. Besides, smaller Micro-LEDs favor a more uniform current spreading, which results in the improved electric characteristics. Thus, the size effect on the sensitivity is investigated by changing the device size from 30  $\mu\text{m}$  to 200  $\mu\text{m}$  at 1 and 100  $\text{mA}/\text{cm}^2$ . The results are displayed in Fig. 3. First, all green Micro-LEDs at 100  $\text{mA}/\text{cm}^2$  show the temperature sensitivity (1.5-1.61  $\text{mV}/\text{K}$ ) close to the ideal sensitivity, 1.57  $\text{mV}/\text{K}$ , indicating the ideal Shockley diode operation at 100  $\text{mA}/\text{cm}^2$ . The temperature sensitivity does not change on size, which is expected from the Shockley diode equation. The temperature sensitivity of the blue and green Micro-LEDs at 1  $\text{mA}/\text{cm}^2$  do not have a clear size dependence. However, for the blue Micro-LED at 100  $\text{mA}/\text{cm}^2$ , the sensitivity increases systematically with increasing size. It could be attributed to a larger series resistance in operation with decreasing size.

Now let's turn our attention to the spectral properties of blue/green InGaN and red AlGaInP Micro-LEDs for display applications. The temperature-dependent EL spectra for blue/green/red Micro-LEDs are displayed in Fig. 4(a), (c), and (e). As temperature increases, the EL peak red-shifted and broadened, and the EL intensity decreases. The emission is generated by electron-hole recombination in the active layer of nitride LEDs, so the band gaps ( $E_g$ ) of the active layers correspond to their EL peaks because of their direct band gap. When temperature increases, the band gap of semiconductors with a direct band gap decreases. It has been understood that the broadening of the energy levels by the lattice vibrations and electron-phonon interaction are responsible for the temperature dependence of band gap of semiconductors.<sup>9,10</sup> The temperature-dependent band gap of the direct semiconductors can be expressed by the semi-empirical Varshni relationship<sup>11</sup>:

$$E_g(T_j) = E_g(0K) - \frac{\alpha T_j^2}{T_j + \beta}$$

where  $E_g(0K)$  is the band gap of the semiconductor at 0 K,  $T_j$  is the junction temperature, and  $\alpha$  and  $\beta$  are fitting parameters characteristic of a given material. The Varshni relation implies that turn-on voltage decreases with increasing temperature. The junction temperature can be estimated from the EL spectra of LEDs because the EL spectrum of LED is dominated by spontaneous emission, and its highest luminescence intensity occurs at<sup>12</sup>

$$E_{g,peak}(T_j) = E_g(T_j) + \frac{1}{2}k_B T_j = E_g(0K) - \frac{\alpha T_j^2}{T_j + \beta} + \frac{1}{2}k_B T_j$$

Thus, the temperature-dependent band gaps of ternary blue and green InGaN, and quaternary  $(\text{Al}_{0.1}\text{Ga}_{0.9})_{0.5}\text{In}_{0.5}\text{P}$  can be calculated by using this equation. We assumed that the cryogenic chamber temperatures of the probe station are not much different from the junction temperature. Fig. 4(b), (d), and (f) displays the calculated band gaps (solid blue lines) for blue/green InGaN and red quaternary  $(\text{Al}_{0.1}\text{Ga}_{0.9})_{0.5}\text{In}_{0.5}\text{P}$ , respectively. The energies of EL peaks corresponding to  $E_g$  agrees relatively well with the calculated  $E_g$ . The narrow FWHMs of Micro-LEDs can lead to a wider color gamut. The FWHMs of blue and green Micro-LEDs range 23-37 nm and 27-41 nm from 300 K to 450 K. The FWHM of red Micro-LED are between 18 and 30 nm in 200-450 K. The spectral shifts of R/G/B Micro-LED by temperature are relatively

small as  $\sim 10$  nm.

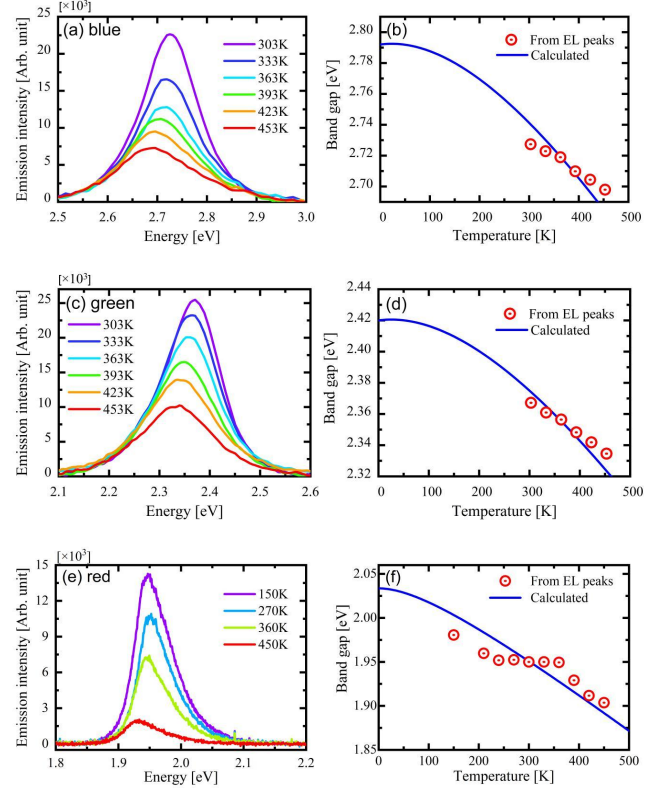


**Fig. 4.** The temperature-dependent electroluminescence spectra, and the band gaps obtained from the EL peaks (red circles) and calculated (blue solid lines).

Specifically, the 1931 CIE ( $x$ ,  $y$ ) chromaticity coordinates are calculated from the EL spectra and are displayed in the 1931 color space as seen in Fig. 5. The  $x$ ,  $y$  values of the color coordinate of R/G/B Micro-LEDs in the CIE1931 increase/decrease with increasing temperature. In particular, all color coordinates of the blue Micro-LEDs in the inset of Fig. 5 are located beyond Rec. 2020 color gamut standard ( $x$ ,  $y=0.131$ ,  $0.046$  for blue), which is the standard color space of ultra-high definition television system.

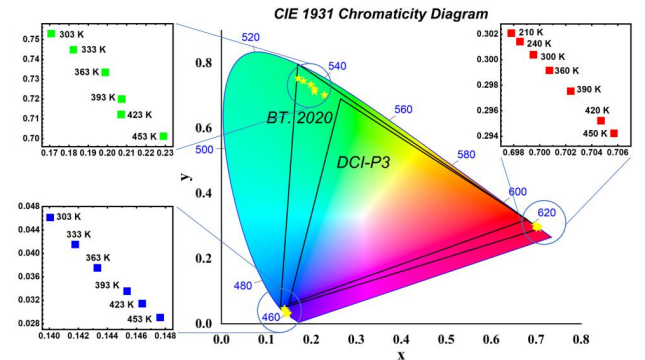


**Fig. 5.** CIE1931 color coordinates of blue/green InGaN and red AlGaInP Micro-LEDs at different temperature.

The color coordinates of green and red Micro-LEDs are also located near Rec. 2020 color gamut standard ( $x$ ,  $y=0.170$ ,  $0.797/0.708$ ,  $0.292$  for green/red) but do not meet completely the requirement of Rec. 2020 standard though they are beyond DCI-

P3 color space ( $x, y=0.265, 0.69/0.68, 0.32$  for green/red), which is an RGB color space introduced in 2007 to cover the color range of cinema and for current ultra-high definition (UHD) premium TVs by the Society of Motion Picture and Television Engineers (SMPTE). However, the color coordinates of the green and red Micro-LEDs at 300 K are quite closely located at the edge of Rec. 2020 color space, indicating our R/G/B Micro-LEDs can have 97% Rec. 2020 color space near 300 K. Even at higher temperatures, our R/G/B Micro-LEDs can cover 170% DCI P3 color space, indicating the stable performance.

## References

- (1) Zhang, K.; Liu, Y.; Kwok, H.; Liu, Z. Investigation Of Electrical Properties And Reliability Of Gan-Based Micro-LEDs. *Nanomaterials* 2020, 10 (4), 689.
- (2) Lu, B.; Wang, Y.; Hyun, B.; Kuo, H.; Liu, Z. Color Difference And Thermal Stability Of Flexible Transparent Ingan/Gan Multiple Quantum Wells Mini-LED Arrays. *IEEE Electron Device Letters* 2020, 1–1.
- (3) Liu, Y.; Zhang, K.; Hyun, B.; Kwok, H.; Liu, Z. High-Brightness Ingan/Gan Micro-Leds With Secondary Peak Effect For Displays. *IEEE Electron Device Letters* 2020, 41 (9), 1380–1383.
- (4) Liu, Z.; Lin, C.; Hyun, B.; Sher, C.; Lv, Z.; Luo, B.; Jiang, F.; Wu, T.; Ho, C.; Kuo, H.; He, J. Micro-Light-Emitting Diodes With Quantum Dots In Display Technology. *Light: Science & Applications* 2020, 9 (1), 1-23.
- (5) Oh, N.; Kim, B. H.; Cho, S.-Y.; Nam, S.; Rogers, S. P.; Jiang, Y.; Flanagan, J. C.; Zhai, Y.; Kim, J.-H.; Lee, J.; Yu, Y.; Cho, Y. K.; Hur, G.; Zhang, J.; Trefonas, P.; Rogers, J. A.; Shim, M. Double-Heterojunction Nanorod Light-Responsive LEDs for Display Applications. *Science* 2017, 355 (6325), 616.
- (6) Ren, B.; Yuen, G.; Deng, S.; Jiang, L.; Zhou, D.; Gu, L.; Xu, P.; Zhang, M.; Fan, Z.; Yueng, F. S. Y.; Chen, R.; Kwok, H.-S.; Li, G. Multifunctional Optoelectronic Device Based on an Asymmetric Active Layer Structure. *Adv. Funct. Mater.* 2019, 29 (17), 1807894.
- (7) Ferreira, R.; Xie, E.; McKendry, J.; Rajbhandari, S.; Chun, H.; Faulkner, G.; Watson, S.; Kelly, A.; Gu, E.; Penty, R.; White, I.; O'Brien, D.; Dawson, M. High Bandwidth GaN-Based Micro-LEDs for Multi-Gb/s Visible Light Communications. *IEEE Photonics Technol. Lett.* 2016, 28 (19), 2023–2026.
- (8) Mansoor, M.; Haneef, I.; Akhtar, S.; De Luca, A.; Udrea, F. Silicon Diode Temperature Sensors—A Review of Applications. *Sens. Actuators Phys.* 2015, 232, 63–74.
- (9) Fan, H. Y. Temperature Dependence of the Energy Gap in Semiconductors. *Phys. Rev.* 1951, 82 (6), 900–905.
- (10) Viña, L.; Logothetidis, S.; Cardona, M. Temperature Dependence of the Dielectric Function of Germanium. *Phys. Rev. B* 1984, 30 (4), 1979–1991.
- (11) Varshni, Y. P. Temperature Dependence of the Energy Gap in Semiconductors. *Physica* 1967, 34 (1), 149–154.
- (12) Bebb, H. B.; Williams, E. W. Chapter 4 Photoluminescence I: Theory; Willardson, R. K., Beer, A. C., Eds.; Semiconductors and Semimetals; Elsevier, 1972; Vol. 8, pp 181–320.